

Continuous-time quantum walks on Erdős-Rényi networks

X.P. Xu^{1,2} and F. Liu²

¹*Institute of High Energy Physics, Chinese Academy of Science, Beijing 100049, China*

²*Institute of Particle Physics, HuaZhong Normal University, Wuhan 430079, China*

(Dated: February 3, 2008)

We study the coherent exciton transport of continuous-time quantum walks (CTQWs) on Erdős-Rényi networks. The Erdős-Rényi network of N nodes is constructed by connecting every pair of nodes with probability p . We numerically calculate the ensemble averaged transition probability of quantum transport between two nodes of the networks. For finite networks, we find that the limiting transition probability is reached very quickly. For infinite networks whose spectral density follows the semicircle law, the efficiencies of the classical and quantum-mechanical transport are compared on networks of different average degree \bar{k} . In the long time limiting, we consider the distribution of the ensemble averaged transition probabilities, and show that there is a high probability to find the exciton at the initial node. Such high return probability almost do not alter in a wide range of connection probability p but increases rapidly when the network approaches to be fully connected. For networks whose topology is not extremely connected, the return probability is inversely proportional to the network size N . Furthermore, the transport dynamics are compared with that on a random graph model in which the degree of each node equals to the average degree \bar{k} of the Erdős-Rényi networks.

PACS numbers: 05.60.Gg, 03.67.-a, 05.40.-a

I. INTRODUCTION

During the last few years, the coherent exciton dynamics in quantum system has been extensively studied by both experimental and theoretical methods [1, 2, 3, 4]. The dynamical behavior of such process depends on the underlying structure of the system under study. Most of previous studies on coherent exciton dynamics are based on simple structures, for example, the line [5, 6], cycle [7, 8], hypercube [9], Cayley tree [10], dendrimers [11], polymers [12] and other regular networks with simple topology. To the best of our knowledge, the dynamics of exciton on random network have not received much attention [13].

In this paper, we consider the coherent exciton transport on random networks of Erdős-Rényi (ER). The coherent exciton dynamics is modeled by continuous-time quantum walks (CTQWs), which is a quantum version of the classical random walk and widely studied by various researchers to describe the relaxation processes in complex systems [14, 15]. In the mathematical literature, the ER random network is defined as follows [16, 17, 18]: Starting with N disconnected nodes, every pair of nodes is connected with probability p ($0 < p < 1$) and multiple connections are prohibited. The ER random network is one of the oldest and best studied models of networks, and possesses the considerable advantage of being exactly solvable for many of its average properties in the limit of large network size [19]. For instance, one interesting feature, which was demonstrated in their original papers, is that the model shows a phase transition with increasing p at which a giant component forms [19, 20]. An alternative and equivalent representation of the ER random graph is to express the graph not in terms of p but in terms of the average degree \bar{k} of the nodes, which is related to the connection probability p as: $\bar{k} = p(N - 1) \approx pN$, where the last approximate equality is hold for large N .

In the limit of large network size N , the degrees of ER random network follow a Poisson distribution peaked at

the average degree \bar{k} . In order to contrast the resemblance and difference of the transport dynamics on networks with the same average degree, we consider the coherent exciton transport on a configuration model of random networks in which the degree k of each node equals to the average degree \bar{k} ($\bar{k} \in \text{Integers}$) of the Erdős-Rényi networks. The method for generating the graph is as follows [21]: one assigns each node \bar{k} ($\bar{k} \in \text{Integers}$) "stubs" -ends of edges emerging from the nodes, and then one chooses pairs of these stubs uniformly at random and joins them together to make complete edges. When all stubs have been used up, the resulting graph is a random member of the ensemble of graphs with the equal degree [19, 21]. The configuration model of random networks can also be implemented by using the edge-interchanging algorithm, which randomly interchange two existing edges while keep the degree sequence unchanged [22, 23]. The configuration model is one of the most successful algorithms proposed for network formation, and has been extensively used as a null model in contraposition to real networks with the same degree distribution in biology, robustness, epidemics spreading and other dynamical processes taking place on complex networks [22, 24, 25]. Here, we adopt this idea to compare the transport behavior on the two network models. As we will show, although the ensembles of ER model and configuration model have the same average number of connections, the transport dynamics on the two models are different.

The paper is structured as follows: In the next section, we briefly review the classical and quantum transport on networks presented in Refs. [26, 27]. In Sec. III we study the time evolution of the ensemble averaged return probability on ER networks with different parameters. Section IV presents the efficiencies of the classical and quantum mechanical transport, and try to reveal how the model parameter affects the transport efficiency. In Sec. V, we consider the distribution of the long time averaged transition probabilities, and explore how the average return probability is related to network parameters. In Sec. VI, we consider the transport dynamics on

extremely connected networks. Conclusions and discussions are given in the last part, Sec. VII.

II. TRANSPORT ON NETWORKS

The coherent exciton dynamics on a connected network is modeled by the continuous-time quantum walks (CTQWs), which is obtained by replacing the Hamiltonian of the system by the classical transfer matrix, $H = -T$ [28]. The transfer matrix T relates to the Laplace matrix by $T = -\gamma A$ [10]. Here, for the sake of simplicity, we assume the transmission rate γ for all connections equals to 1. The Laplace matrix A has non-diagonal elements A_{ij} equal to -1 if nodes i and j are connected and 0 otherwise. The diagonal elements A_{ii} equal to the number of total links connected to node i , i.e., A_{ii} equals to the degree of node i . The states $|j\rangle$ endowed with the nodes j of the network form a complete, ortho-normalised basis set, which span the whole accessible Hilbert space, i.e., $\sum_k |k\rangle\langle k| = 1$, $\langle k|j\rangle = \delta_{kj}$. The transport processes are governed by the master equation or Schrödinger equation [10]. The classical and quantum mechanical transition probabilities to go from the state $|j\rangle$ at time 0 to the state $|k\rangle$ at time t are given by $p_{k,j}(t) = \langle k|e^{-tA}|j\rangle$ and $\pi_{k,j}(t) = |\alpha_{k,j}(t)|^2 = |\langle k|e^{-itH}|j\rangle|^2$ [10], respectively. Generally speaking, to calculate the transition probabilities, all the eigenvalues and eigenvectors of the transfer operator and Hamiltonian are required. We use E_n to represent the n th eigenvalue of H and denote the orthonormalized eigenstate of Hamiltonian by $|q_n\rangle$, such that $\sum_n |q_n\rangle\langle q_n| = 1$. The classical and quantum transition probabilities between two nodes can be written as,

$$p_{k,j}(t) = \sum_n e^{-tE_n} \langle k|q_n\rangle\langle q_n|j\rangle, \quad (1)$$

and

$$\begin{aligned} \pi_{k,j}(t) &= |\alpha_{k,j}(t)|^2 \\ &= \sum_{n,l} e^{-it(E_n - E_l)} \\ &\quad \times \langle k|q_n\rangle\langle q_n|j\rangle\langle j|q_l\rangle\langle q_l|k\rangle. \end{aligned} \quad (2)$$

The above equations give the general expressions of the classical and quantum transition probabilities, which explicitly depends on the eigenvalues and eigenvectors of the transfer matrix or Hamiltonian. A particular feature related to the transport is the return probability, which is the probability of finding the exciton at the initial node. The transition probability depends on the specific topology of the generated single network, therefore it is appropriate to consider its ensemble averages.

III. AVERAGED RETURN PROBABILITIES

The average of the classical and quantum return probabilities $p_{j,j}(t)$ and $\pi_{j,j}(t)$ over all nodes of the network are

$$\begin{aligned} \bar{p}(t) &= \frac{1}{N} \sum_n e^{-tE_n} \sum_j \langle q_n|j\rangle\langle j|q_n\rangle \\ &= \frac{1}{N} \sum_n e^{-tE_n}, \end{aligned} \quad (3)$$

and

$$\begin{aligned} \bar{\pi}(t) &= \frac{1}{N} \sum_j \pi_{j,j}(t) = \frac{1}{N} \sum_j |\alpha_{j,j}(t)|^2 \\ &= \frac{1}{N} \sum_{n,l} e^{-it(E_n - E_l)} \\ &\quad \times \sum_j \langle j|q_n\rangle\langle q_n|j\rangle\langle j|q_l\rangle\langle q_l|j\rangle. \end{aligned} \quad (4)$$

The classical $\bar{p}(t)$ is only dependent on the eigenvalues and decays monotonically from $\bar{p}(0) = 1$ to the equipartition $\lim_{t \rightarrow \infty} \bar{p}(t) = 1/N$. The quantum $\bar{\pi}(t)$ is dependent on the eigenvalues and eigenvectors, which is cumbersome in the numerical calculations. The above equations present the average of return probabilities over all nodes on a specific single network. In order to reduce the statistical fluctuation, we further average the return probabilities over distinct single networks, i.e.,

$$\langle \bar{p}(t) \rangle = \frac{1}{R} \sum_{r=1}^R \bar{p}^r(t), \quad (5)$$

and

$$\langle \bar{\pi}(t) \rangle = \frac{1}{R} \sum_{r=1}^R \bar{\pi}^r(t), \quad (6)$$

where the index r denotes the r th generated ER network. Throughout this paper, we denote the average over network nodes by a bar (e.g., \bar{k} , $\bar{p}(t)$, $\bar{\pi}(t)$, etc.), and the average over different realizations by a bracket (e.g., $\langle \bar{p}(t) \rangle$) while the actual values by undecorated characters.

Figure 1(a) shows the ensemble averaged return probabilities $\langle \bar{p}(t) \rangle$ and $\langle \bar{\pi}(t) \rangle$ on ER networks of size $N = 100$ with average degree $\bar{k} = 10, 20$ and 30. For classical transport $\langle \bar{p}(t) \rangle$ reaches the equipartition $\lim_{t \rightarrow \infty} \bar{p}(t) = 1/N$ very quickly. The curves at intermediate times follow stretched exponential decay, which differs from power law decay ($t^{-0.5}$) for the cycle graph [29]. The exponential decay of $\langle \bar{p}(t) \rangle$ indicates that a classical excitation will quickly spread the whole network and occupy each node with a uniform probability $1/N$ in a short time. It is evident that the excitation reaches the equipartition $1/N$ more quickly on networks with more connections (compare the curves in Fig. 1(a)). For quantum transport $\langle \bar{\pi}(t) \rangle$ also decays quickly in the intermediate times and then reach a final plateau. This plateau is larger than the equipartitioned probability $1/N$. After a careful examination, we find such plateau corresponds to a constant value $\langle \bar{\pi}(t) \rangle \approx 0.065 \pm 0.01$. Increasing the average degree \bar{k} nearly does not change this value (compare the curves in Fig. 1(a)). We note that here $\langle \bar{\pi}(t) \rangle$ is smooth and does not display the oscillatory behavior, in contrast to the case for the cycle graph in which the return probability shows a quasi-periodic pattern [29]. The non-periodic behavior of $\langle \bar{\pi}(t) \rangle$ may be attributed to the large connectivity of the networks consider here.

In Fig. 1(b), we show the same plot of $\langle \bar{p}(t) \rangle$ and $\langle \bar{\pi}(t) \rangle$ on a random graph model in which the degrees of each node are exactly equal to $k = 10, 20$ and 30. The behavior of $\langle \bar{p}(t) \rangle$ is almost the same as that on the ER networks. However, $\langle \bar{\pi}(t) \rangle$ is quite different. $\langle \bar{\pi}(t) \rangle$ oscillates at intermediate times and also reaches a constant value. Such constant value (0.028 ± 0.003) is lower

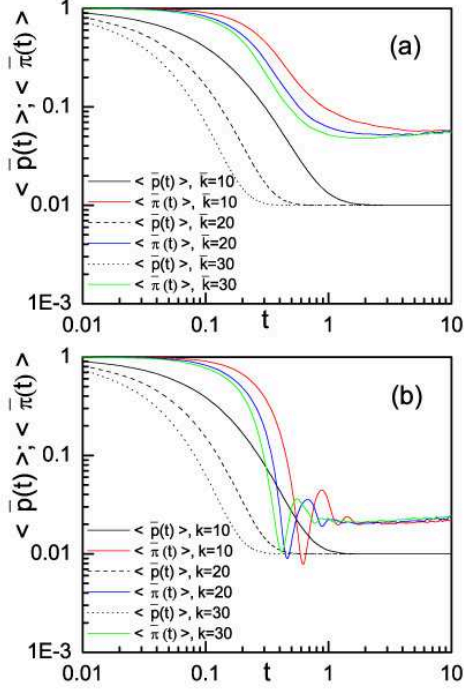


FIG. 1: (Color online) Averaged return probabilities $\langle \bar{p}(t) \rangle$ and $\langle \bar{\pi}(t) \rangle$ for random networks generated by the ER model (a) and configuration model (b) with different values of degree. The networks are of size $N = 100$ and the (average) degree of the networks are $\bar{k} = 10$, $\bar{k} = 20$ and $\bar{k} = 30$ (see the different line styles), respectively. All the curves are averaged over 100 independent realizations.

than that of the ER networks but larger than that of the cycle graph ($(2N - 2)/N^2 = 0.0198$ for even-numbered networks and $(2N - 1)/N^2 = 0.0199$ for odd-numbered networks) [30]. The random networks generated by the ER model and configuration model have the same number of total connections (on average), but the average return probabilities are quite different. Such difference may be caused by the different ensembles generated by the network models.

IV. EFFICIENCY OF TRANSPORT ON INFINITE NETWORKS

On finite networks, both the classical and quantum return probabilities do not decay ad infinitum but reach a constant value at some time [29]. This value is related to the size of the networks. To reveal the decay behavior at large time scales, we consider $\langle \bar{p}(t) \rangle$ and $\langle \bar{\pi}(t) \rangle$ on infinite networks. In this case, the spectrum density can be regarded as a continuous distribution. Because the networks considered here are uncorrelated random networks [31], the spectral density of the Laplacian Matrix converges to the semicircular distribution,

$$\rho(E) = \begin{cases} \frac{\sqrt{4\sigma^2 - (E - \bar{k})^2}}{2\pi\sigma^2}, & \text{if } |E - \bar{k}| < 2\sigma, \\ 0, & \text{Otherwise.} \end{cases} \quad (7)$$

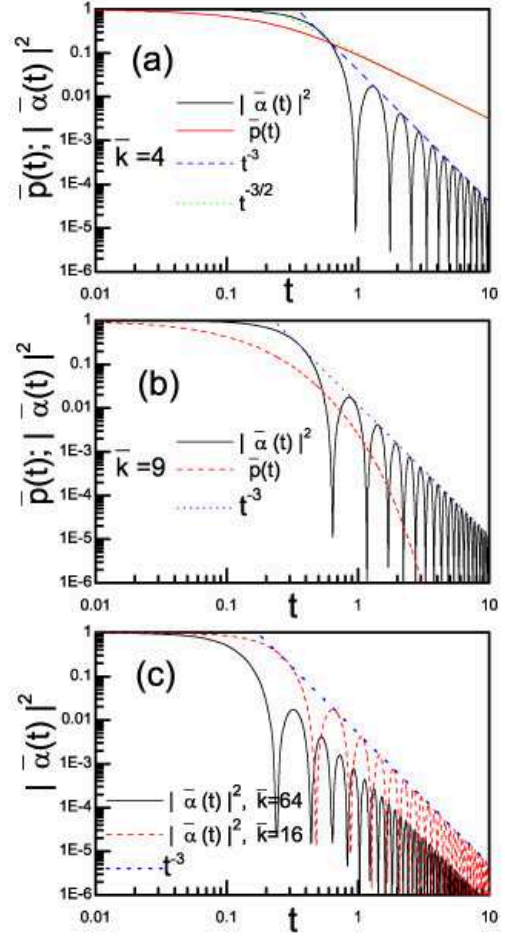


FIG. 2: (Color online) Efficiency of the classical and quantum transport. (a) Time evolution of $\bar{p}(t)$ and $|\bar{\alpha}(t)|^2$ for $\bar{k} = 4$. Both the classical and quantum transport at long time scales show the power law behavior. The exponent of local maxima of $|\bar{\alpha}(t)|^2$ is twice the exponent of $\bar{p}(t)$, implying the quantum transport is more efficient than the classical one. (b) Time evolution of $\bar{p}(t)$ and $|\bar{\alpha}(t)|^2$ for $\bar{k} = 9$. Here, $\bar{p}(t)$ drops below $|\bar{\alpha}(t)|^2$ and shows an exponential decay. Thus for $\bar{k} = 9$ the classical transport is more efficient than the quantum one. (c) $|\bar{\alpha}(t)|^2$ versus t for $\bar{k} = 64$ and $\bar{k} = 16$. The curve depresses vertically on highly connected networks, suggesting that the quantum transport becomes more efficient when the connectivity of network increases.

Where $\sigma = \sqrt{Np(1-p)}$ and $\bar{k} = p(N-1)$ for the ER networks [32]. This theorem is also known as Wigners law [33], and it has extensive applications in statistical physics, solid-state physics and complex quantum-mechanical systems [34, 35].

For sparse networks, i.e., $p \ll 1$, σ^2 can be simplified as $\sigma^2 \approx \bar{k}$. Thus Eq. (7) can be written as,

$$\rho(E) = \begin{cases} \frac{\sqrt{4\bar{k} - (E - \bar{k})^2}}{2\pi\bar{k}}, & \text{if } |E - \bar{k}| < 2\sqrt{\bar{k}}, \\ 0, & \text{Otherwise.} \end{cases} \quad (8)$$

Therefore the spectral density is only a function of the average degree \bar{k} on large sparsely connected networks. Using the above expression, we can calculate the return

probabilities of Eqs. (3) and (4) in the continuum limit as follows,

$$\bar{p}(t) = \int e^{-tE} \rho(E) dE = \int \frac{e^{-tE} \sqrt{4\bar{k} - (E - \bar{k})^2}}{2\pi\bar{k}} dE, \quad (9)$$

and

$$\begin{aligned} \bar{\pi}(t) &\geq \left| \frac{1}{N} \sum_n e^{-itE_n} \right|^2 \equiv |\bar{\alpha}(t)|^2, \\ |\bar{\alpha}(t)|^2 &= \left| \int e^{-itE} \rho(E) dE \right|^2 \\ &= \left| \int \frac{e^{-itE} \sqrt{4\bar{k} - (E - \bar{k})^2}}{2\pi\bar{k}} dE \right|^2 \end{aligned} \quad (10)$$

Where the lower bound is obtained by using the Cauchy-Schwarz inequality and exact for regular networks [26]. Analogous to the classical case, $|\bar{\alpha}(t)|^2$ depends only on the eigenvalues of the Hamiltonian. Although $|\bar{\alpha}(t)|^2$ is a lower bound and differs from the exact value $\bar{\pi}(t)$, $|\bar{\alpha}(t)|^2$ quantitatively reproduce the overall behavior of $\bar{\pi}(t)$ [29]. Therefore it is appropriate to use the decay of $|\bar{\alpha}(t)|^2$ to measure the efficiency of the quantum transport [29].

Fig. 2 shows the temporal behavior of $\bar{p}(t)$ and $|\bar{\alpha}(t)|^2$ according to Eqs. (9) and (10) for different values of average degree \bar{k} . For $\bar{k} = 4$ (Fig. 1(a)), $\bar{p}(t)$ scales as $\bar{p}(t) \sim t^{-1.5}$ and the local maxima of $|\bar{\alpha}(t)|^2$ scales as $|\bar{\alpha}(t)|^2 \sim t^{-3}$ at long times. Such scaling argument can be understood by the spectral density. When $\bar{k} = 4$, the spectral density becomes as $\rho(E) = \sqrt{8E - E^2}/8\pi$. The long time behavior of $\bar{p}(t)$ and $|\bar{\alpha}(t)|^2$ are mainly determined by small E values, thus we can assume $\rho(E) \sim \sqrt{E}$ [29]. Such scaling behavior leads to the power law behavior of the return probabilities, where the exponent for the quantum transport is twice the exponent of its classical counterpart [29].

The behavior of $\bar{p}(t)$ and $|\bar{\alpha}(t)|^2$ alters accordingly when the average degree \bar{k} increases. In Fig. 2(b), we show $\bar{p}(t)$ and $|\bar{\alpha}(t)|^2$ for $\bar{k} = 9$. Now the classical $\bar{p}(t)$ does not show scaling but displays an exponential decay. We note that $\bar{p}(t)$ decays faster than $|\bar{\alpha}(t)|^2$, this indicates that the classical excitation spreads over the network faster than the quantum one. As a matter of fact, we find that for networks with $\bar{k} > 4$, $\bar{p}(t)$ always shows a faster decay at long times compared to $|\bar{\alpha}(t)|^2$. Such a behavior indicates that the classical transport is more efficient than the quantum transport on networks with large average degree.

The behavior $|\bar{\alpha}(t)|^2$ is qualitatively the same when the average degree \bar{k} increases. To incarnate the difference of $|\bar{\alpha}(t)|^2$, we plot $|\bar{\alpha}(t)|^2$ as a function of t for $\bar{k} = 16$ and $\bar{k} = 64$ in Fig. 2(c). As we can see, the local maxima of $|\bar{\alpha}(t)|^2$ scales as $|\bar{\alpha}(t)|^2 \sim t^{-3}$ for both the values of \bar{k} . However, the scaling depresses vertically for large \bar{k} . This vertical depression of $|\bar{\alpha}(t)|^2$ suggests that the quantum transport becomes more efficient when the network connectivity increases.

We note that the increase of average degree greatly changes the efficiency of the classical transport. This is ascribed to large value of the eigenvalues E for network with large average degree. For large \bar{k} , $\bar{p}(t)$ decays exponentially, in contrast to the power law decay for small \bar{k} . Quantum mechanically, the increase of average degree does not change the power law behavior of the local maxima of $|\bar{\alpha}(t)|^2$, but the first minimum is reached quickly and the local maxima of $|\bar{\alpha}(t)|^2$ become lower on highly connected networks.

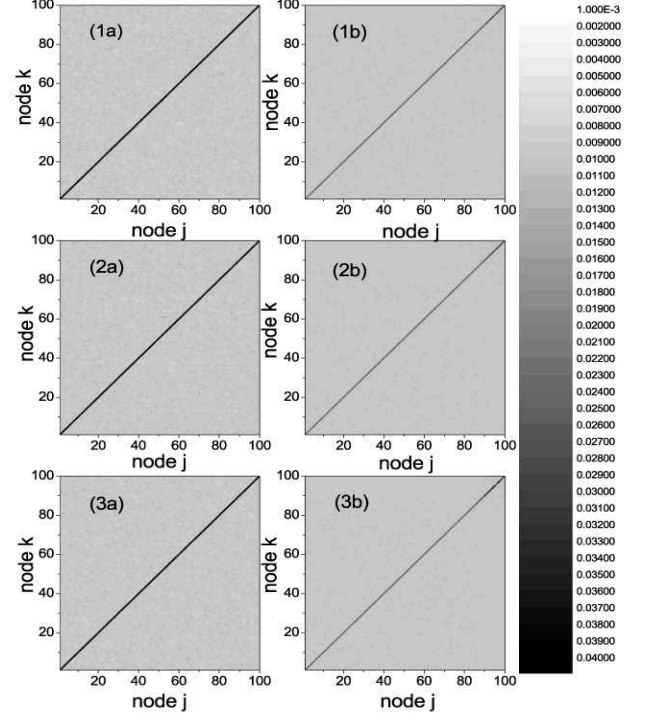


FIG. 3: (Coloronline) Ensemble averaged transition probability $\langle \chi_{k,j} \rangle$ for random networks generated by the ER model (column (a)) and configuration model (column (b)) with different values of degree 10, 20 and 30 (rows 1-3). The network size is $N = 100$ and the average is over 100 realizations. The colormap is shown in the right hand of the plot. Dark regions denote large values of $\langle \chi_{k,j} \rangle$ and bright regions low values of $\langle \chi_{k,j} \rangle$.

V. LONG TIME AVERAGES

On finite networks, the transition probability converges to a certain value, this value is determined by the long time average. Classically, the long time averaged transition probability equals to the equal-partitioned probability $1/N$. However, the quantum mechanical transport does not lead to equipartition. Taking into account the ensemble average, we have,

$$\begin{aligned} \langle \chi_{k,j} \rangle &= \langle \lim_{T \rightarrow \infty} \frac{1}{T} \int_0^T \pi_{k,j}(t) dt \rangle \\ &= \langle \left(\sum_{n,l} \langle k|q_n \rangle \langle q_n|j \rangle \langle k|q_l \rangle \langle q_l|j \rangle \right. \\ &\quad \times \left. \lim_{T \rightarrow \infty} \frac{1}{T} \int_0^T e^{-it(E_n - E_l)} dt \right) \rangle \\ &= \langle \left(\sum_{n,l} \delta(E_n - E_l) \langle k|q_n \rangle \langle q_n|j \rangle \right. \\ &\quad \times \left. \langle k|q_l \rangle \langle q_l|j \rangle \right) \rangle. \end{aligned} \quad (11)$$

Where $\delta(E_n - E_l) = 1$ for $E_n = E_l$ and $\delta(E_n - E_l) = 0$ else. Here, we numerically calculate the ensemble averaged transition probabilities according to the above equation. The results are shown in Fig. 3. The dark regions denote large values of $\langle \chi_{k,j} \rangle$ and bright regions low values of $\langle \chi_{k,j} \rangle$. The dark blocks in the diagonal positions correspond to the large return probability. To view the quantitative behavior of $\langle \chi_{k,j} \rangle$, we plot the distribution of $\langle \chi_{k,j} \rangle$ between all the pairs of two nodes in Fig. 4. The peaks in Fig. 4(a) correspond to the non-diagonal transition probabilities while

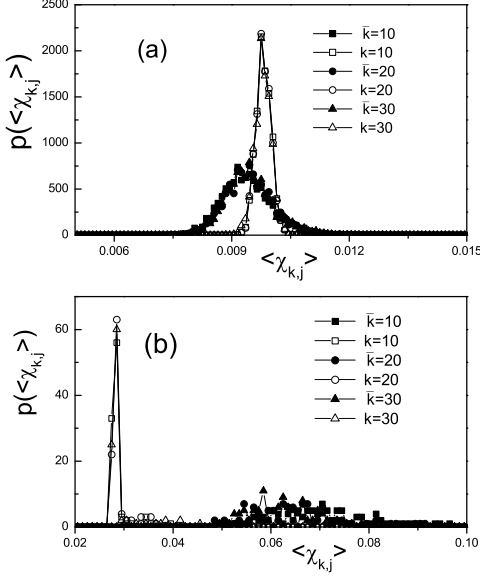


FIG. 4: Distribution of ensemble averaged transition probability $\langle \chi_{k,j} \rangle$ in the region $0.005 < \chi_{k,j} < 0.015$ (a) and $0.02 < \chi_{k,j} < 0.1$ (b). The k with and without bar presents the random graphs generated by the ER model and configuration model, respectively. The peaks in (a) are from the non-diagonal transition probabilities and the peaks in (b) corresponds to the return probabilities.

the peaks in Fig. 4(a) correspond to the return probabilities [13]. The solid symbols denote the results for the ER networks, and the hollow symbols denote the numerical results for the random graphs generated by the configuration model where the degrees are exactly equal to the average degree of ER networks. It is observed that mean value of the non-diagonal transition probability for the ER model is smaller than that for the configuration model (see Fig. 4(a)). A contrary conclusion for the return probability is demonstrated in Fig. 4(b). We also find that the increase of degree does not change the central values of the peaks (compare the different symbols in the figure). This suggests that the quantum transition probabilities may do not change greatly when connectivity of the networks increases [13]. In order to reveal how the return probability is related to the average degree, we show both the node and ensemble averaged return probability ($\langle \bar{\chi} \rangle = \langle \sum_j \chi_{j,j} / N \rangle$) in Fig. 5(a). As we can see, the average return probability $\langle \bar{\chi} \rangle$ is almost a constant value in a wide range of average degree \bar{k} but increases drastically when the network approaches to be fully connected [13]. Here, the difference for the two random graph models is also visible. The saturated value $\langle \bar{\chi} \rangle$ of the ER networks is larger than that of the random graphs generated by the configuration model. In addition, we have also studied the relationship of the average return probability $\langle \bar{\chi} \rangle$ and the network size N , which is shown in Fig. 5(b). It is found that the averaged return probability $\langle \bar{\chi} \rangle$ is inversely proportional to the network size N (see the asymptote indicated in the figure). This means that the return probability of small-size networks is larger than that of large-size networks.

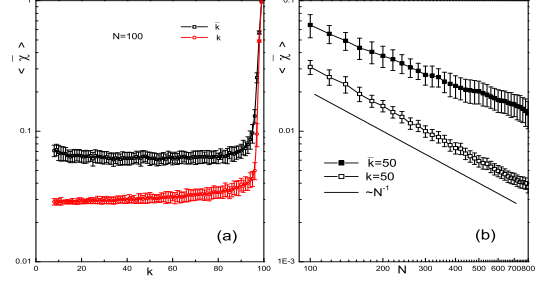


FIG. 5: Average return probability $\langle \bar{\chi} \rangle$ on random networks generated by the ER model (marked by \bar{k}) and configuration model (marked by k). (a) $\langle \bar{\chi} \rangle$ versus k on networks of size $N = 100$. (b) $\langle \bar{\chi} \rangle$ versus network size N when the degree equals to 50.

VI. TRANSPORT ON EXTREMELY CONNECTED NETWORKS

As we have shown, the average return probability $\langle \bar{\chi} \rangle$ increases rapidly when the networks approach to be fully connected. To study this issue in detail, we consider the transport on extremely connected networks. In such case, the connection probability p approaches to 1 and the degree of the network is of the order $\mathcal{O}(N)$. We construct the extremely connected networks by randomly removing a certain number of edges on the fully connected network. The resulting network is equivalent to the ER random network, and the algebra of removing edges is much computationally cheaper than the ER random graph algebra.

Here, we consider the transport on networks of size $N = 100$, and assume the number of removed edges is m . Fig. 6 shows the average return probability $\langle \bar{\chi} \rangle$ as a function of the number of removed edges. We note that $\langle \bar{\chi} \rangle$ decreases to ~ 0.1 when only 4% edges (200 edges) are removed. As more and more edges removed, $\langle \bar{\chi} \rangle$ decreases slowly and tends to reach the saturated value ~ 0.65 . We find that the $\langle \bar{\chi} \rangle$ versus m can be well described by an exponential decay $\langle \bar{\chi} \rangle \sim e^{-0.014m}$ in the region $m < 200$. When only a few edges are removed, $\langle \bar{\chi} \rangle$ is close to the return probability of the complete network (or fully connected network). For a fully connected network of size N , one eigenvalue of the Hamiltonian is 0 and all the other values are equal to N , the long time averaged return probability is $\bar{\chi} = (N^2 - 2N + 2)/N^2$. This is a striking feature of CTQWs which differs from the classical counterpart.

VII. CONCLUSIONS AND DISCUSSIONS

In conclusion, we have studied the classical and quantum transport on Erdős-Rényi networks. We numerically calculate the ensemble averaged transition probability between two nodes of the networks. For finite networks, we find that the limiting transition probability is reached very quickly. For infinite networks whose spectral density follows the semicircle law, the efficiencies of the classical and quantum mechanical transport

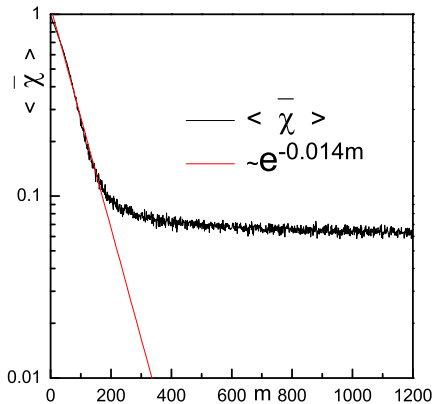


FIG. 6: (Color online) Average return probability $\langle \bar{\chi} \rangle$ versus the number of removed edges m on networks of size $N = 100$. The straight line indicates the exponential decay for $m < 200$.

are compared on networks of different average degree \bar{k} . It is shown that the classical transport is more efficient than the quantum transport on networks with large connectivity. In the long time limiting, we consider the distribution of the ensemble averaged transition probability, and show that the quantum transport exhibits a high re-

turn probability. Such high return probability almost do not change in a wide range of connection probability p but increases rapidly when the network approaches to be fully connected. For networks whose topology is not extremely connected, the return probability is inversely proportional to the network size N . In addition, we also compare the results with that on a random graph model in which the degree of each node equals to the average degree \bar{k} of the Erdős-Rényi networks.

We have shown that the transport dynamics on the ER networks is different from that on the equivalent network generated by the configuration model. The difference may be related to the different ensembles of the network model. Since the return probability reflects the symmetry of the network structure, the high return probability on ER networks may suggest a high symmetry of the topology [36].

Acknowledgments

The authors would like to thank Zhu Kai for converting the mathematical package used in the calculations. This work is supported by the Cai Xu Foundation for Research and Creation (CFRC), National Natural Science Foundation of China under project 10575042 and MOE of China under contract number IRT0624 (CCNU).

-
- [1] J. Feldmann, et al., Phys. Rev. Lett. **70**, 3027 (1993).
 - [2] T. Stroucken, A. Knorr, P. Thomas, and S. W. Koch, Phys. Rev. B **53**, 2026(1996).
 - [3] M. Dyakonov, et al., Phys. Rev. B **56**, 10412 (1997)
 - [4] G. R. Allan and H. M. van Driel, Phys. Rev. B **59**, 15740 (1999).
 - [5] N. Ashwin and V. Ashvin, quant-ph/0010117.
 - [6] G. Abal, R. Siri, A. Romanelli, et al., Phys. Rev. A **73**, 042302(2006).
 - [7] D. Solenov and L. Fedichkin, Phys. Rev. A **73**, 012313(2003).
 - [8] F. Sorrentino, M. di Bernardo, G. H. Cuéllar, and S. Boccaletti, Physica D **224**, 123 (2006).
 - [9] H. Krovi and T. A. Brun, Phys. Rev. A **73**, 032341 (2006).
 - [10] O. Mülken and A. Blumen, Phys. Rev. E **71**, 016101 (2005).
 - [11] O. Mülken, V. Bierbaum and A. Blumen, J. Chem. Phys **124**, 124905 (2006).
 - [12] W. Barford and C. D. P. Duffy, Phys. Rev. B **74** 075207 (2006).
 - [13] O. Mülken, V. Pernice and A. Blumen, Phys. Rev. E **76**, 051125 (2007).
 - [14] Y. Aharonov, L. Davidovich, and N. Zagury, Phys. Rev. A **48**, 1687 (1993).
 - [15] N. Shenvi, J. Kempe, and K. Brigitta Whaley, Phys. Rev. A **67**, 052307 (2003).
 - [16] P. Erdős and A. Rényi, Publicationes Mathematicae **6**, 290 (1959)
 - [17] P. Erdős and A. Rényi, Publications of the Mathematical Institute of the Hungarian Academy of Sciences **5**, 17(1960).
 - [18] P. Erdős and A. Rényi, Acta Mathematica Scientia Hungaria **12**, 26 (1961).
 - [19] M. E. J. Newman, cond-mat/0202208.
 - [20] R. Albert and A.-L. Barabási, Rev. Mod. Phys **74**, 47 (2002).
 - [21] M. E. J. Newman, SIAM Review, **45**, 167 (2003).
 - [22] R. Milo et al., Science, **303**, 1538 (2004).
 - [23] B. J. Kim et al., Phys. Rev. E **69**, 045101 (2004).
 - [24] S. Maslov and K. Sneppen, Science **296**, 910 (2002).
 - [25] M. E. J. Newman, Phys. Rev. Lett **95**, 108701 (2005).
 - [26] A. Volta, O. Mülken and A. Blumen, J. Phys. A **39**, 14997 (2006).
 - [27] O. Mülken, A. Volta and A. Blumen, Phys. Rev. A **72**, 042334 (2005).
 - [28] E. Farhi and S. Gutmann, Phys. Rev. A **58**, 915 (1998).
 - [29] O. Mülken and A. Blumen, Phys. Rev. E **73**, 066117 (2006).
 - [30] O. Mülken and A. Blumen, Phys. Rev. A **73**, 012105 (2006).
 - [31] I. J. Farkas et al., Phys. Rev. E **64**, 026704 (2001).
 - [32] B. Gong, L. Yang and K. Yang, Phys. Rev. E **72**, 037101 (2005).
 - [33] E. P. Wigner, Ann. Math **62**, 548 (1955); **65**, 203 (1957); **67**, 325 (1958).
 - [34] M. L. Mehta, *Random Matrices* (2nd ed, Academic, New York, 1991).
 - [35] A. Crisanti, G. Paladin and A. Vulpiani, *Products of Random Matrices in Statistical Physics* (Springer Series in Solid-State Sciences Vol. 104 Springer, Berlin, 1993).
 - [36] Y. Xiao et al., arXiv:0709.1249.